Biointerface Research in Applied Chemistry
Platinum Open Access Journal (ISSN: 2069-5837)

Article
Volume 11, Issue 5, 2021, 12796 - 12807
https://doi.org/10.33263/BRIAC115.1279612807

Vibrational Analysis and Molecular Docking Studies on some Ribonuclease-H HIV Inhibitors

Prashasti Sinha [1], Anwesh Pandey [1], Anil Kumar Yadav [1,*]

[1] Department of Physics, School for Physical & Decision Sciences, Babasaheb Bhimrao Ambedkar University, Lucknow-226025 Uttar Pradesh; India prsinha2451@gmail.com (P.S.); apdapbbau@gmail.com (A.P.); anilkyadava@bbau.ac.in (A.K.Y.);
* Correspondence: anilkyadava@bbau.ac.in;

Scopus Author ID 57190871447

Received: 17.12.2020; Revised: 15.01.2021; Accepted: 20.01.2021; Published: 31.01.2021

Abstract: Ribonuclease-H (RNase-H) enzyme of the human immunodeficiency virus (HIV) reverse transcriptase (RT) shows inhibitory activity with novel galloyl derivatives having enzymatic assays of IC_{50} S at sub to low micromolar concentration. The computational analysis of these stated galloyl derivatives was carried out in order to extract information and performance with the target proteins. The compounds N-hydroxylisoquinolinediones (HID), β-thujaplicinol, diketoacid, diketoacid ester, pyrimidinol carboxylic acids, naphthyridinones, 3hydroxypyrimidine-2,4-dione (HPD), and hydroxypyridonecarboxylic acids are the selected galloyl derivatives of human immunodeficiency virus-I (HIV-I) RNase-H active site inhibitors that were optimized using Turbomole software. Further evaluation of their NMR shielding of the stated compounds was performed using B3-LYP hybrid functional, and the def-SV basis set was carried out from the same software. These optimized compounds were then docked to targets (PDB Id: 5EGA and 3K2P) using AutoDock 4 software. After analyzing the docking result, Hydroxylisoquinoline and Naphthyridinones give better binding results with both the targets.

Keywords: galloyl derivatives; HIV-I; molecular docking; RNase-H Inhibitors.

1. Introduction

Infectious diseases may be due to an organism's body tissues' attack by several causative agents undergoing multiplication and interacting with host tissues to produce toxins [1,2]. Infective agents may of various types like viruses, bacteria, fungi, parasites, arthropods, etc. Some pathogens interact with host nucleic acid using reverse transcriptase that is an anomaly of life's central dogma [3,4]. Certain viruses are taking the route of infecting the host's genetic code and utilizing the host enzymes and raw materials for their growth, like the human immunodeficiency virus (HIV). The Human Immunodeficiency Viruses are species of two lentiviruses that belongs to a retrovirus subgroup. It causes HIV infection, and gradually with the passage of time, it turns to Acquired Immunodeficiency Syndrome (AIDs) [5,6]. Vital cells such as Helper T-cells ($CD4^+$ T-cells), macrophages, and dendritic cells of the human immune system are mainly infected by HIV [7]. Reduced $CD4^+$ T-cells are observed from HIV infections. Below a critical level of CD4+ T-cells, there is a reduction in the immunity levels regulated by cells thus making the body vulnerable to infections, ultimately leading to AIDs development in the body [8].

HIV comes from Retroviridae [9], a member of the genus Lentiviruses [10]. Lentiviruses have several similar biological properties and morphologies. Species that are infected by Lentiviruses results in long term illness along with an incubation period of long duration [11]. The transmission mechanism of Lentiviruses is observed through a positive-sense RNA virus; these RNA are single-stranded. As it enters the target cell with the help of an enzyme that is virally encoded, reverse transcriptase, a single-stranded viral RNA genome is reverse transcribed into a double-stranded DNA. The new viral DNA is imported to the cell nucleus, and with the help of an enzyme integrase that is virally encoded, it is then integrated into cellular DNA of the host [12]. After integration, the virus may remain dormant for some time, avoiding detection its and by the host's defense mechanism [13]. This virus can remain latent inside the host for a very long period after the initial exposure of infection. Significantly, no manifestations of the disease can be observed. Alternatively, the DNA infected by the virus gets transcribed into a new genomic sequence producing a new viral RNA followed by the production of a viral protein with the usage of enzymes produced in the host cell, this procedure is followed by the packaging and release of the material from the cell. This material then participates in the process of replication and allowing itself to multiply.

Several mechanisms for the spreading of HIV participate in the ongoing virus's replication despite antiretroviral therapies [14,15]. According to WHO, HIV is one of the most common diseases spreading widely in all nations, but patients with AIDs are comparatively rare. Several antiretroviral drugs are used for the management of HIV/AIDs. Antiviral medications are specifically used for the treatment of viral infections [16]. Genomes constitute viruses and few enzymes stored in protein in a capsule structure covered with lipid layer. The propagation of viruses is observed by subjugating host cells and producing replicas of themselves; hence that is for the next generation. The viral life cycle depends on the virus type: The host cell attaches, the release of virus-infected genes and infected virus in the host cell, using host cell machinery the viral components replicates, such viral components assemble to form viral particles, these viral particles are released in the new host cells in order to infect the cell and continue the spread phenomena.

Highly active antiretroviral therapy (HAART) is the terminology used for multiple drugs acting on different virus targets. This maintains immunity and opportunistic infections, which leads to death [17]. Specifically, these are major classifications of drugs used under various combinations to cure HIV infection. Antiretroviral drugs are classified based on the retrovirus life cycle inhibited by the chemical compound. They are namely Nucleoside Reverse Transcriptase Inhibitors (NRTIs) as long as a backbone, accompanied by a Non-Nucleoside Reverse Transcriptase Inhibitors (NNRTIs), the Protease Inhibitors (PI), the Integrase Inhibitors (II) and Reverse Transcriptase (RT)-associated Ribonuclease H (RNase H). The HIV-1 Ribonuclease H shows inhibitory activity with galloyl derivatives; these derivatives are Hydroxylisoquinoline, β-thujaplicinol, diketoacid, diketoacid ester, pyrimidinol carboxylic acids, naphthyridinones, 3-hydroxypyrimidine-2,4-dione (HPD), and hydroxypyridonecarboxylic acids [18].

In this research work, to study the inhibitory activity, molecular docking is performed. Their respective results were analyzed to generate stable complexes. Molecular docking predicts the best dock poses and gives fine details of docking score and binding site energy [19]. Thus, in the field of drug discovery, in silico approach plays a vital role. Here fig.1 shows the chemical structure of galloyl derivatives.

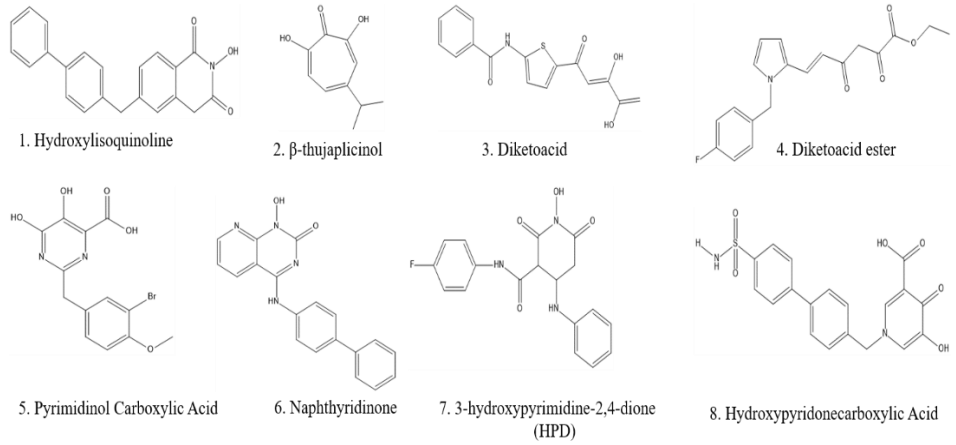

Figure 1. 2D structure of the galloyl derivatives of Ribonuclease H HIV inhibitors.

2. Materials and Methods

2.1. Geometry optimization.

This is the process using with the molecule finds its configuration in minimum energy [20]. The procedure starts with the calculation of wave function and the energy at the beginning, which then proceeds with the search of the new geometry of lower energy. The visualization of the 2D structures of Ribonuclease H HIV-1 inhibitors' derivatives was done with ChemDraw software for a better understanding of the atoms and the bonds participating in the molecule formation. These molecules were drawn on Avogadro software [21].

The molecules' PDB files were used as the input files in TmoleX software [22] where its electronic and vibrational analysis were conducted. The optimization of the molecule was done by setting the basis set as B3-LYP/def-SV(P) [23] and commanding it to perform the optimization to obtain the molecule in its minimum energy state.

2.2. Molecular docking.

Molecular docking was performed with the help of AutoDock software[24]. For docking simulations, one needs the target molecule which will bind with the ligand. The need for the target protein was fulfilled by the Protein Data Bank[25]. With the help of this database site, two target molecules were obtained: 5EGA and 3K2P. Target (PDB Id: 5EGA) is a protein of 187 amino acids and is a suitable target for the drugs of H1N1 viruses. On the other hand, the target (PDB Id: 3K2P) is a protein suitable for HIV 1 and HIV 2 drugs.

The target file was extended to UCSF Chimera software [26], and there, the previously docked ligands were removed with the available commands on the software. The target was then ready to be docked again with the new ligand. Using the AutoDock 4 software [24], the target was inserted, and water molecules were removed. The polar hydrogen atoms were added, followed by the addition of Kollman charges and Gasteirger charges [27]. The output file is extended to the UCSF Chimera software; it shows the 3D docked complex formed by the ligand's docking with the target macromolecule. Further evaluation of the interactions taking place between the ligand and the target macromolecule is studied using Ligplot^{+} [28]; this software ensures that the user gets the 2D structure of docked complex where all the interactions (mainly concerned with the hydrogen bonds) between ligand and the active residues of the target. The observations were recorded for the detailed study of the docked complexes.

3. Results and Discussion

3.1. Geometry optimization.

The optimized molecules' results were extracted from the output file of TmoleX software shown below in table 1. To make the work more convenient, each compound was referred to as ligand 1, ligand 2, ligand 3, ligand 4, ligand 5, ligand 6, ligand 7, ligand 8, respectively, for the sake of convenience. Fig. 2 shows the optimized geometries of all the selected ligands.

Table 1. Calculation of energies of the compounds using TmoleX software.

Compound	Zero Point Vibrational Energy (Hartree)	Enthalpy (KJ mol^{-1})	Free Energy (KJ mol^{-1})	HOMO LUMO Gap (eV)
Ligand 1	0.3167	-1126.1119	-1126.4283	0.459
Ligand 2	0.1466	-610.4612	-610.6079	0.770
Ligand 3	0.2370	-1399.4946	-1399.5120	0.237
Ligand 4	0.2366	-1185.4186	-1185.6552	0.356
Ligand 5	0.1561	-3557.2410	-3557.3971	0.539
Ligand 6	0.2343	-1136.2504	-1136.4847	0.243
Ligand 7	0.2033	-1254.2398	-1254.4432	0.377
Ligand 8	0.2265	-1687.1337	-1687.3602	0.254

The above calculations were carried out using turbomol software keeping:

- B3-LYP/def-SV(P) in symmetry C1
- At temperature 298.15K and pressure 0.1P

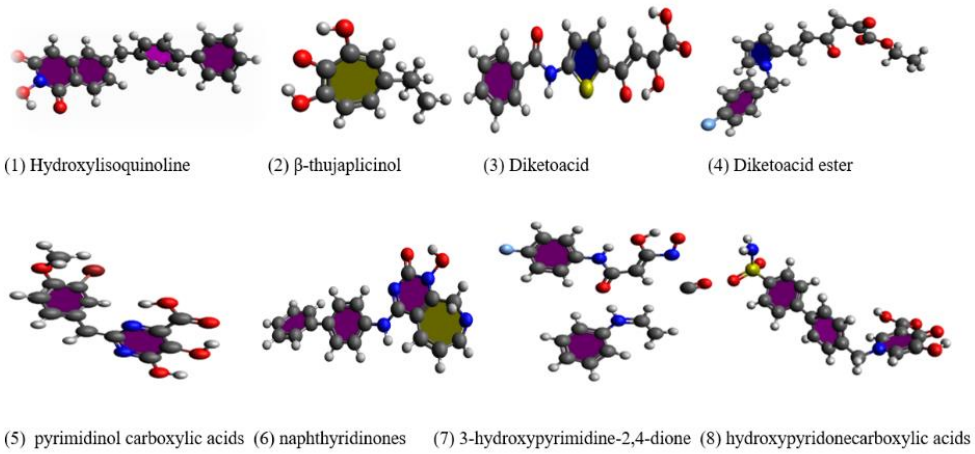

Figure 2. The optimized geometrical structures of the selected ligands.

Table 2. The evaluation of energies obtained through NMR shielding.

Compound	Kinetic Energy (KJ mol^{-1})	Potential Energy (KJ mol^{-1})	Total Energy (KJ mol^{-1})
Ligand 1	1116.6519	-2243.4146	-1126.7627
Ligand 2	604.7809	-1215.3888	-610.6079
Ligand 3	1391.2364	-2790.7485	-1399.5121
Ligand 4	1170.4720	-2356.1273	-1185.6552
Ligand 5	3541.7823	-7099.1794	-3557.3971
Ligand 6	1123.5304	-2260.0152	-1136.4847
Ligand 7	1242.9068	-2497.3500	-1254.4432
Ligand 8	1677.4081	-3364.7684	-1687.3602

Further, the Infrared activity and Raman activity of the selected ligands were computed based on the output files of each molecule's vibrational analysis of each molecule overall frequencies. It was observed that all the eight ligands were both IR and Raman active. This

shows the bulk molecular system has a similar identity element but has dissimilar symmetry that is the absence of a center of symmetry. Lastly, the estimation of NMR shielding evaluated the kinetic energy and the molecule's potential energy again using similar software [29]. Results that were evaluated from NMR shielding: Kinetic energy, Potential energy, and Total energy are mentioned in table 2, shown below.

Above calculations were carried out using turbomol software for NMR shielding keeping: B3-LYP/def-SV(P) in symmetry C1; at temperature 298.15K and pressure 0.1P.

3.2. Molecular docking.

The results obtained on docking all the eight ligands with target 1 (PDB Id: 5EGA) and target 2 (PDB Id: 3K2P) respectively [30,31] are shown below in figures 3 & 4, respectively. Table 3 represents the different types of interacting residues obtained during the docking calculations in the selected ligands' vicinity with both the targets.

Docking with Target-1: (PDB Id: 5EGA)

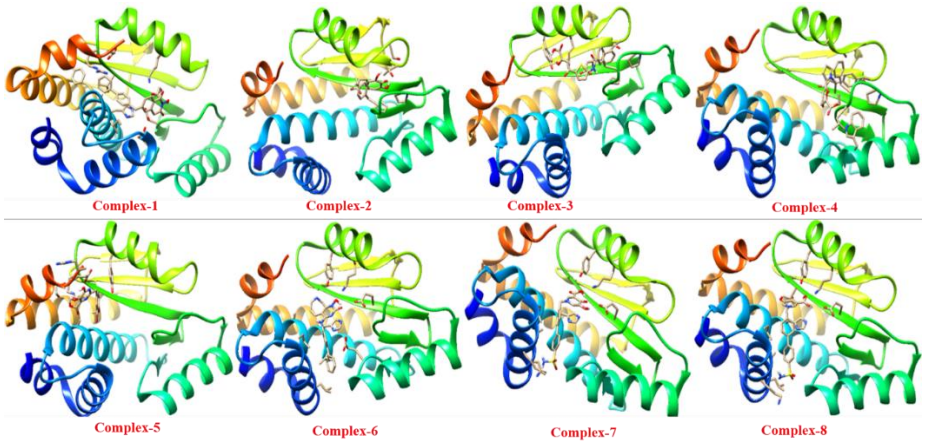

Figure 3. The 3D docked posed structure of the selected ligands with target-1 (5EGA).

Docking with Target-2:(PDB Id: 3K2P)

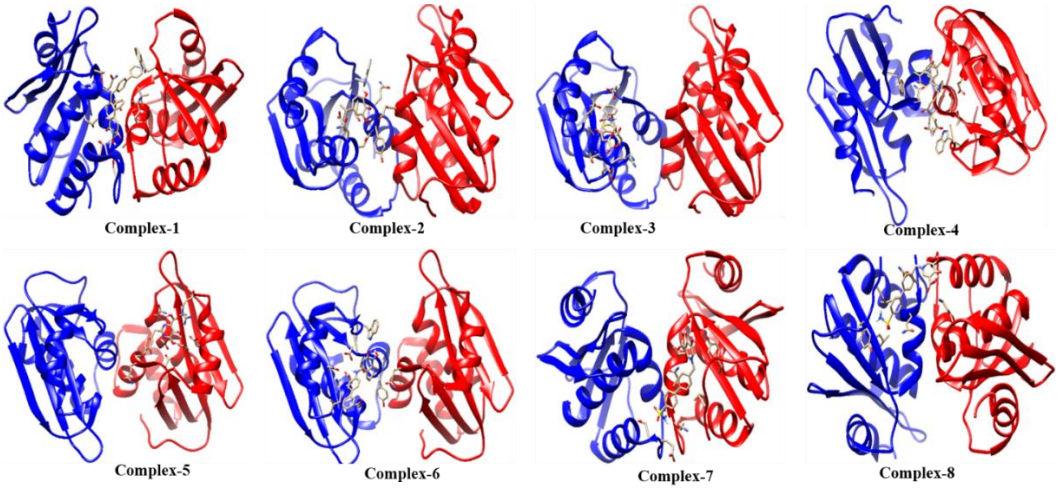

Figure 4. The 3D docked posed structure of the selected ligands with target-2 (3K2P).

Further, subsequent to docking calculations, each target's binding affinities with every ligand were noted, and a graph was plotted based on the results. The binding affinity for both targets is mentioned in table 3, and a comparative graph representing is shown in fig. 5.

Table 3. Binding affinities of the selected ligands with both the targets.

Selected Ligands	Target-1 (PDB Id: 5EGA)	Target-2 (PDB Id: 3K2P)
Ligand 1	-7.25 kcal/mol	-7.12 kcal/mol
Ligand 2	-5.83 kcal/mol	-5.72 kcal/mol
Ligand 3	-6.86 kcal/mol	-6.42 kcal/mol
Ligand 4	-6.43 kcal/mol	-5.76 kcal/mol
Ligand 5	-6.08 kcal/mol	-5.77 kcal/mol
Ligand 6	-9.05 kcal/mol	-7.99 kcal/mol
Ligand 7	-7.54 kcal/mol	-7.07 kcal/mol
Ligand 8	-6.94 kcal/mol	-8.31 kcal/mol

The two targets can be compared based on their binding affinities

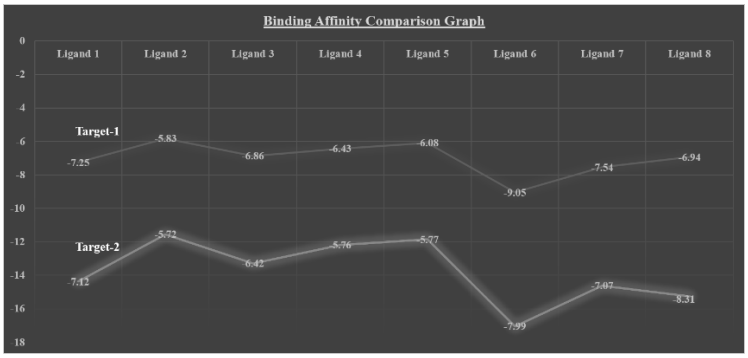

Figure 5. Graph representing variations in binding affinities for both targets.

3.3. Hydrogen bond analysis.

After studying the docked complex, the ligand's interaction with the active residues of the target was drawn with the help of Ligplot+ software [34]. The interaction, such as hydrogen bonding between the ligand atoms and the active residues, can be seen from figures 6 & 7, as shown below, followed by hydrophobic interactions with the target's active residues [32,33]. Also, table 4 & table 5, shown below, represent the residues involved in hydrogen bond formation and hydrophilic interactions followed by hydrogen bond lengths in Table 6.

Interactions with Target-1:(PDB Id: 5EGA)

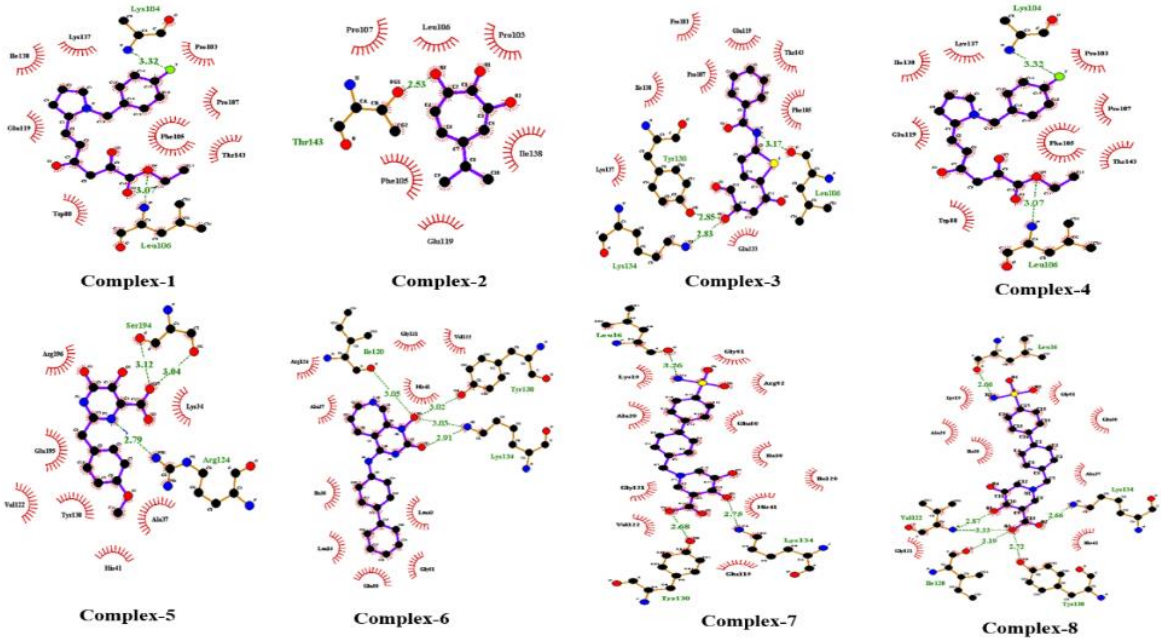

Figure 6. The hydrogen interactions of the selected ligands with target-1 (5EGA).

Interactions with Target-2:(PDB Id: 3K2P)

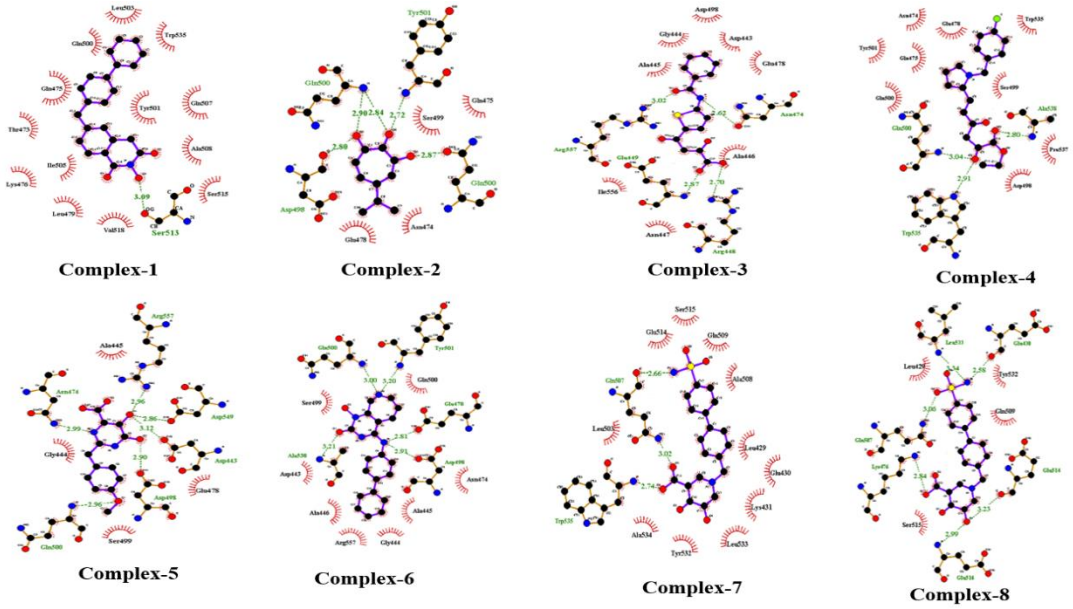

Figure 7. The hydrogen interactions of the selected ligands with target-2 (3K2P).

Table 4. Hydrogen bond and hydrophobic interaction residues of target-1 (PDB ID 5EGA).

Ligand	**Interactions**	
	Hydrogen bonds	**Hydrophobic Interactions**
Ligand 1	Lys 134 Leu 106	Glu 195 Ala 37 Phe 150 Val 122 His 41 Arg 124 Thr 123 Pro 107 Glu 119 Glu 80 Asp 108
Ligand 2	Thr 143	Pro 107 Leu 106 Pro 103 Phe 105 Ile 138 Glu 119
Ligand 3	Leu 106 Tyr 130 Lys 134	Pro 103 Ile 138 Pro 107 Glu 119 Thr 143 Phe 105 Lys 137 Glu 133
Ligand 4	Lys 104 Leu 106	Ile 138 Lys 137 Pro 103 Pro 107 Glu 119 Phe 105 Trp 88 Thr 143
Ligand 5	Ser 194 Ser 194 Arg 124	Arg 196 Lys 34 Glu 195 Val 122 Tyr 130 Ala 37 His 41
Ligand 6	Ile 120 Tyr 130	Arg 124 Gly 121

Ligand	Interactions	
	Hydrogen bonds	**Hydrophobic Interactions**
	Lys 134 Lys 134	Val 122 Ala 37 His 41 Ile 38 Leu 42 Leu 16 Glu 80 Gly 81
Ligand 7	Leu 16 Lys 134 Tyr 130	Lys 19 Gly 81 Ala 20 Arg 82 Glu 80 Ile 38 Gly 121 Val 122 Ile 120 His 41 Glu 119
Ligand 8	Leu 16 Lys 134 Val 122 Val 122 Ile 120 Tyr 130	Lys 19 Ala 20 Ile 38 Gly 81 Glu 80 Ala 37 Gly 121 His 41

Table 5. Hydrogen bond and hydrophobic interaction residues of target-2 (PDB ID 3K2P).

Ligand	Interactions	
	Hydrogen bonds	**Hydrophobic Interactions**
Ligand 1	Ser 513	Leu 503 Gln 500 Trp 535 Gln 475 Tyr 501 Gln 507 Thr 473 Lys 476 Ile 505 Ala 508 Leu 479 Val 518 Ser 515
Ligand 2	Tyr 501 Gln 500 Asp 498 Gln 500	Ser 499 Gln 475 Glu 478 Asn 474
Ligand 3	Arg 557 Asn 474 Glu 449 Arg 448	Asp 498 Gly 444 Ala 445 Asp 443 Glu 478 Ile 556 Ala 446 Asn 447
Ligand 4	Gln 500 Trp 535 Ala 538	Tyr 501 Asn 474 Gln 500 Gln 475 Glu 478 Trp 535 Ser 499 Pro 537 Asp 498
Ligand 5	Asn 474 Arg 557	Ala 445 Gly 444

Ligand	Interactions	
	Hydrogen bonds	**Hydrophobic Interactions**
	Asp 549 Asp 443 Asp 498 Gln 500	Glu 478 Ser 499
Ligand 6	Gln 500 Tyr 501 Ala 538 Asp 498 Glu 478	Ser 4499 Gln 500 Asp 443 Ala 446 Arg 557 Gly 444 Ala 445 Asn 474
Ligand 7	Gln 507 Gln 507 Trp 535	Glu 514 Ser 515 Gln 509 Ala 508 Leu 503 Leu 429 Glu 430 Lys 431 Leu 533 Tyr 532 Ala 534
Ligand 8	Leu 533 Glu 430 Gln 507 Lys 476 Glu 516 Glu 514	Leu 429 Tyr 532 Gln 509 Ser 515

Table 6. The bond length of H-bonds of all the ligands with both the targets.

Ligand	Target-1 (PDB ID: 5EGA)	Target-2 (PDB ID: 3K2P)
Ligand 1	Lys 134 – 3.32 Å Leu 106–3.07 Å	Ser 513–3.09 Å
Ligand 2	Thr 143 – 2.53 Å	Tyr 501– 2.72 Å Gln 500– 2.90 Å Asp 498– 2.80 Å Gln 500– 2.84 Å
Ligand 3	Leu 106 – 3.17 Å Tyr130 – 2.85 Å Lys 134 – 3.83 Å	Arg 557– 3.02 Å Asn 474– 2.62 Å Glu 449– 2.87 Å Arg 448– 2.70 Å
Ligand 4	Lys 104 – 3.32 Å Leu 106 – 3.07 Å	Gln 500 – 3.04 Å Trp 535 – 2.91 Å Ala 538– 2.80 Å
Ligand 5	Ser 194 – 3.12 Å Ser 194 – 3.04 Å Arg 124 – 2.79 Å	Asn 474 – 2.99 Å Arg 557 – 2.96 Å Asp 549 – 2.86 Å Asp 443 – 3.12 Å Asp 498 – 2.90 Å Gln 500– 2.96 Å
Ligand 6	Ile 120 – 3.05 Å Tyr 130 – 3.02 Å Lys 134 – 3.03 Å Lys 134 – 2.91 Å	Gln 500 – 3.00 Å Tyr 501 – 3.20 Å Ala 538 – 3.21 Å Asp 498 – 2.91 Å Glu 478– 2.81 Å
Ligand 7	Leu 16 – 3.26 Å Lys 134 – 2.68 Å Tyr 130 – 2.75 Å	Gln 507 – 2.66 Å Gln 507 – 3.02 Å Trp 535– 2.74 Å
Ligand 8	Leu 16 – 2.66 Å Lys 134 – 2.66 Å Val 122 – 2.87 Å Val 122 – 3.33 Å Ile 120 – 3.19 Å Tyr 130 – 2.72 Å	Leu 533 – 3.34 Å Glu 430 – 2.58 Å Gln 507 – 3.06 Å Lys 476 – 2.84 Å Glu 516 – 2.99 Å Glu 514– 3.23 Å

Docking study performed in order to estimate protein binding affinities of ligands. The observed binding energy values [35-38] of some Ribonuclease inhibitors such as β-thujaplicinol, diketoacid, diketoacid ester, pyrimidinol carboxylic acids, and 3hydroxypyrimidine-2,4-dione was found to be -4.60 kcal/mol, -6.31 kcal/mol, -5.48 kcal/mol, -5.84 kcal/mol and -7.0 kcal/mol while the calculated value was -5.72 kcal/mol, -6.42 kcal/mol, -5.76 kcal/mol, -5.77 kcal/mol and -7.07 kcal/mol respectively. Thus the experimental trend is successfully followed by the theoretical binding energies [39, 40]. Such studies have proven themselves to be of significant importance regarding the evaluation of drugs' stability with the dynamics of biomolecules [41, 42]. This theoretical evaluation will help in the improvement of existing ribonucleic inhibitors. It will also prove to be supportive in designing some novel HIV drugs.

4. Conclusions

Considering the geometry optimization results, ligand 5 that is pyrimidinol carboxylic acid, is the most stable compound. As it has the lowest bond enthalpy, which means it has a high tendency to form bonds with any target. Further, analyzing all the docked complexes' output files, ligand 6, i.e., naphthyridinones found to be the best-docked molecule with target 5EGA. Therefore, the study revealed that ligand 5 that is pyrimidinol carboxylic acids is the most stable compound. Further, ligand 1 is Hydroxylisoquinoline, and ligand 6 is naphthyridinones docked with the target (PDB Id: 5EGA and PDB Id: 3K2P) forms the favorable docked complex, which has the highest binding affinity compared to the other derivatives. This may result in the formation of other enzymatic complexes, which will be highly beneficial for inhibiting the Human Immuno Virus into the host body. This study also fulfills its aim of complementing the experimental studies on ribonuclease-H HIV inhibitors and adds to the database on its computational studies.

Funding

This research received no external funding.

Acknowledgments

Prashasti Sinha would like to acknowledge Prof. Devesh Kumar for discussions and help, and would also like to thank the Head, Department of Physics, Babasaheb Bhimrao Ambedkar University for permitting the use of laboratory and facilities of the department.

Conflicts of Interest

The authors declare no conflict of interest.

References

1. Paris, G.; Picaud, F. On the perfect diameter condition to optimize the antibiotic nanoencapsulation: case of gramicidin. *Letters in Applied NanoBioScience* **2019**, *8*, 654-660, https://doi.org/10.33263/LIANBS83.654660.
2. P Pottie, K.; Girard, V. Common Infectious Diseases. *Primary Care: Clinics in Office Practice* **2020**, https://doi.org/10.1016/j.pop.2020.11.002.
3. Al-Azzam, S.; Ding, Y.; Liu, J.; Pandya, P.; Ting, J.P.; Afshar, S. Peptides to combat viral infectious diseases. *Peptides* **2020**, *134*, https://doi.org/10.1016/j.peptides.2020.170402.

4. Rocha, S.; Hendrix, J.; Borrenberghs, D.; Debyser, Z.; Hofkens, J. Imaging the Replication of Single Viruses: Lessons Learned from HIV and Future Challenges To Overcome. *ACS Nano* **2020**, *14*, 10775-10783, https://doi.org/10.1021/acsnano.0c06369.
5. Sperk, M.; van Domselaar, R.; Rodriguez, J.E.; Mikaeloff, F.; Sá Vinhas, B.; Saccon, E.; Sönnerborg, A.; Singh, K.; Gupta, S.; Végvári, Á.; Neogi, U. Utility of Proteomics in Emerging and Re-Emerging Infectious Diseases Caused by RNA Viruses. *Journal of Proteome Research* **2020**, *19*, 4259-4274, https://doi.org/10.1021/acs.jproteome.0c00380.
6. Fromentin, R.; Chomont, N. HIV persistence in subsets of CD4+ T cells: 50 shades of reservoirs. *Seminars in Immunology* **2020**, 1044-5323, https://doi.org/10.1016/j.smim.2020.101438.
7. Song, N.; Sengupta, S.; Khoruzhenko, S.; Welsh, R.A.; Kim, A.; Kumar, M.R.; Sønder, S.U.; Sidhom, J.-W.; Zhang, H.; Jie, C.; Siliciano, R.F.; Sadegh-Nasseri, S. Multiple genetic programs contribute to CD4 T cell memory differentiation and longevity by maintaining T cell quiescence. *Cellular Immunology* **2020**, *357*, https://doi.org/10.1016/j.cellimm.2020.104210.
8. Terahara, K.; Iwabuchi, R.; Iwaki, R.; Takahashi, Y.; Tsunetsugu-Yokota, Y. Substantial induction of non-apoptotic CD4 T-cell death during the early phase of HIV-1 infection in a humanized mouse model. *Microbes and Infection* **2020**, https://doi.org/10.1016/j.micinf.2020.10.003.
9. Ruggiero, E.; Tassinari, M.; Perrone, R.; Nadai, M.; Richter, S.N. Stable and Conserved G-Quadruplexes in the Long Terminal Repeat Promoter of Retroviruses. *ACS Infectious Diseases* **2019**, *5*, 1150-1159, https://doi.org/10.1021/acsinfecdis.9b00011.
10. Kayirangwa, E.; Hanson, J.; Munyakazi, L.; Kabeja, A. Current trends in Rwanda's HIV/AIDS epidemic. *Sexually Transmitted Infections* **2006**, *82*, http://dx.doi.org/10.1136/sti.2006.019588.
11. Konrad, B.P.; Taylor, D.; Conway, J.M.; Ogilvie, G.S.; Coombs, D. On the duration of the period between exposure to HIV and detectable infection. *Epidemics* **2017**, *20*, 73-83, https://doi.org/10.1016/j.epidem.2017.03.002.
12. Zennou, V.; Petit, C.; Guetard, D.; Nerhbass, U.; Montagnier, L.; Charneau, P. HIV-1 Genome Nuclear Import Is Mediated by a Central DNA Flap. *Cell* **2000**, *101*, 173-185, https://doi.org/10.1016/S0092-8674(00)80828-4.
13. Kallings, L.O. The first postmodern pandemic: 25 years of HIV/ AIDS. *Journal of internal medicine* **2008**, *263*, 218-243, https://doi.org/10.1111/j.1365-2796.2007.01910.x.
14. Talbert-Slagle, K.; Atkins, K.E.; Yan, K.-K.; Khurana, E.; Gerstein, M.; Bradley, E.H.; Berg, D.; Galvani, A.P.; Townsend, J.P. Cellular Superspreaders: An Epidemiological Perspective on HIV Infection inside the Body. *PLoS Pathog* **2014**, *10*, https://doi.org/10.1371/journal.ppat.1004092.
15. Bago, J.-L.; Lompo, M.L. Exploring the linkage between exposure to mass media and HIV awareness among adolescents in Uganda. *Sexual & Reproductive Healthcare* **2019**, *21*, 1-8, https://doi.org/10.1016/j.srhc.2019.04.004.
16. Zang, X.; Krebs, E.; Wang, L.; Marshall, B.D.L.; Granich, R.; Schackman, B.R.; Montaner, J.S.G.; Nosyk, B.; Behrends, C.N.; Del Rio, C.; Dombrowski, J.; Feaster, D.J.; Gebo, K.; Golden, M.; Granich, R.; Kerr, T.; Kirk, G.; Marshall, B.D.L.; Mehta, S.H.; Metsch, L.; Montaner, J.S.G.; Nosyk, B.; Schackman, B.R.; Shoptaw, S.; Small, W.; Strathdee, S.; the Localized, H.I.V.m.s.g. Structural Design and Data Requirements for Simulation Modelling in HIV/AIDS: A Narrative Review. *PharmacoEconomics* **2019**, *37*, 1219-1239, https://doi.org/10.1007/s40273-019-00817-1.
17. Woolf-King, S.E.; Sheinfil, A.Z.; Ramos, J.; Foley, J.D.; Moskal, D.; Firkey, M.; Kellen, D.; Maisto, S.A. A conceptual model of alcohol use and adherence to antiretroviral therapy: systematic review and theoretical implications for mechanisms of action. *Health Psychology Review* **2020**, 1–68, https://doi.org/10.1080/17437199.2020.1806722.
18. Tramontano, E.; Corona, A.; Menéndez-Arias, L. Ribonuclease H, an unexploited target for antiviral intervention against HIV and hepatitis B virus. *Antiviral Research* **2019**, *171*, https://doi.org/10.1016/j.antiviral.2019.104613.
19. Mohammadhassan, R.; Fallahi, S.; Mohammadalipour, Z. ADMET and pharmaceutical activity analysis of caffeic acid diversities by in silico tools. *Letters in Applied NanoBioScience* **2020**, *9*, 840-848, https://doi.org/10.33263/LIANBS91.840848.
20. van Lenthe, E.; Ehlers, A.; Baerends, E.-J. Geometry optimizations in the zero order regular approximation for relativistic effects. *The Journal of Chemical Physics* **1999**, *110*, 8943-8953, http://dx.doi.org/10.1063/1.478813.
21. Hanwell, M.D.; Curtis, D.E.; Lonie, D.C.; Vandermeersch, T.; Zurek, E.; Hutchison, G.R. Avogadro: an advanced semantic chemical editor, visualization, and analysis platform. *Journal of Cheminformatics* **2012**, *4*, https://doi.org/10.1186/1758-2946-4-17.
22. Steffen, C.; Thomas, K.; Huniar, U.; Hellweg, A.; Rubner, O.; Schroer, A. TmoleX--a graphical user interface for TURBOMOLE. *J Comput Chem* **2010**, *31*, 2967-2970.
23. Hrovat, D.; Williams, R.; Goren, A.; Borden, W. B3LYP calculations on bishomoaromaticity in substituted semibullvalenes. *Journal of Computational Chemistry* **2001**, *22*, 1565-1573, https://doi.org/10.1002/jcc.1110.

24. Morris, G.M.; Huey, R.; Lindstrom, W.; Sanner, M.F.; Belew, R.K.; Goodsell, D.S.; Olson, A.J. AutoDock4 and AutoDockTools4: Automated docking with selective receptor flexibility. *J Comput Chem* **2009**, *30*, 2785-2791.
25. Berman, H.; Henrick, K.; Nakamura, H. Announcing the worldwide Protein Data Bank. *Nature Structural & Molecular Biology* **2003**, *10*, 980-980, https://doi.org/10.1038/nsb1203-980.
26. Pettersen, E.F.; Goddard, T.D.; Huang, C.C.; Couch, G.S.; Greenblatt, D.M.; Meng, E.C.; Ferrin, T.E. UCSF Chimera--a visualization system for exploratory research and analysis. *J Comput Chem* **2004**, *25*, 1605-1612, https://doi.org/10.1002/jcc.20084.
27. Yadav, P.; Sharma, B.; Sharma, C.; Singh, P.; Awasthi, S.K. Interaction between the Antimalarial Drug Dispiro-Tetraoxanes and Human Serum Albumin: A Combined Study with Spectroscopic Methods and Computational Studies. *ACS Omega* **2020**, *5*, 6472-6480, https://doi.org/10.1021/acsomega.9b04095.
28. Wallace, A.C.; Laskowski, R.A.; Thornton, J.M. LIGPLOT: a program to generate schematic diagrams of protein-ligand interactions. *Protein Engineering, Design and Selection* **1995**, *8*, 127-134, https://doi.org/10.1093/protein/8.2.127.
29. Borgsmiller, K.L.; O'Connell, D.J.; Klauenberg, K.M.; Wilson, P.M.; Stromberg, C.J. Infrared and Raman Spectroscopy: A Discovery-Based Activity for the General Chemistry Curriculum. *Journal of Chemical Education* **2012**, *89*, 365-369, https://doi.org/10.1021/ed2002835.
30. Lee, I.; Il Kim, J.; Park, S.; Bae, J.-Y.; Yoo, K.; Yun, S.-H.; Lee, J.-Y.; Kim, K.; Kang, C.; Park, M.-S. Single PA mutation as a high yield determinant of avian influenza vaccines. *Scientific Reports* **2017**, *7*, https://doi.org/10.1038/srep40675.
31. D'Erasmo, M.P.; Masaoka, T.; Wilson, J.A.; Hunte, E.M.; Beutler, J.A.; Le Grice, S.F.J.; Murelli, R.P. Traceless solid-phase α-hydroxytropolone synthesis. *MedChemComm* **2016**, *7*, 1789-1792, https://doi.org/10.1039/c6md00237d.
32. Cui, X.; Liu, J.; Xie, L.; Huang, J.; Zeng, H. Interfacial ion specificity modulates hydrophobic interaction. *Journal of Colloid and Interface Science* **2020**, *578*, 135-145, https://doi.org/10.1016/j.jcis.2020.05.091.
33. Alekseeva, I.V.; Kuznetsova, A.A.; Bakman, A.S.; Fedorova, O.S.; Kuznetsov, N.A. The role of active-site amino acid residues in the cleavage of DNA and RNA substrates by human apurinic/apyrimidinic endonuclease APE1. *Biochimica et Biophysica Acta (BBA) - General Subjects* **2020**, *1864*, https://doi.org/10.1016/j.bbagen.2020.129718.
34. Galindo-Murillo, R.; Aguilar-Suárez, L.E.; Barroso-Flores, J. A mixed DFT-MD methodology for the in silico development of drug releasing macrocycles. Calix and thia-calix[N]arenes as carriers for Bosutinib and Sorafenib. *Journal of Computational Chemistry* **2016**, *37*, 940-946, https://doi.org/10.1002/jcc.24281.
35. Zhang, B.; D'Erasmo, M.P.; Murelli, R.P.; Gallicchio, E. Free Energy-Based Virtual Screening and Optimization of RNase H Inhibitors of HIV-1 Reverse Transcriptase. *ACS Omega* **2016**, *1*, 435-447, https://doi.org/10.1021/acsomega.6b00123.
36. Sirous, H.; Zabihollahi, R.; Aghasadeghi, M.R.; Sadat, S.M.; Saghaie, L.; Fassihi, A. Docking studies of some 5-hydroxypyridine-4-one derivatives: evaluation of integrase and ribonuclease H domain of reverse transcriptase as possible targets for anti-HIV-1 activity. *Medicinal Chemistry Research* **2015**, *24*, 2195-2212, https://doi.org/10.1007/s00044-014-1289-1.
37. Vora, J.; Patel, S.; Sinha, S.; Sharma, S.; Srivastava, A.; Chhabria, M.; Shrivastava, N. Molecular docking, QSAR and ADMET based mining of natural compounds against prime targets of HIV. *Journal of Biomolecular Structure and Dynamics* **2019**, *37*, 131-146,https://doi.org/10.1080/07391102.2017.1420489.
38. Mostoufi, A.; Chamkouri, N.; Kordrostami, S.; Alghasibabaahmadi, E.; Mojaddami, A. 3-Hydroxypyrimidine-2,4-dione derivatives as HIV Reverse Transcriptase-Associated RNase H Inhibitors: QSAR analysis and molecular docking studies. *Iranian Journal of Pharmaceutical Research* **2020**, *19*, 84-97, https://doi.org/10.22037/IJPR.2020.1101004.
39. Moghadam, S.A.; Preto, J.; Klobukowski, M.; Tuszynski, J.A. Testing amino acid-codon affinity hypothesis using molecular docking. *Biosystems* **2020**, *198*, https://doi.org/10.1016/j.biosystems.2020.104251.
40. Shinoda, Y.; Wang, Y.; Yamamoto, T.; Miyachi, H.; Fukunaga, K. Analysis of binding affinity and docking of novel fatty acid-binding protein (FABP) ligands. *Journal of Pharmacological Sciences* **2020**, *143*, 264-271, https://doi.org/10.1016/j.jphs.2020.05.005.
41. Pandey, A.; Yadav, R. ; Shukla, A. ; Yadav, A.K. Unveiling the Antimicrobial Activities of Dicationic Carbazoles and Related Analogs Through Computational Docking. *Adv Sci Eng Med*. **2020**, *12*, 40-44, https://doi.org/10.1166/asem.2020.2513.
42. Pandey, A. ; Upadhyaya, A. ; Kumar, S. ; Yadav, A.K. Interaction, Dynamics and Stability Analysis of Some Minor Groove Binders With B-DNA Dodecamer 5'-(CGCAAATTTGCG)-3'. *Drug Des*. **2020**, *10*, 172, https://10.35248/2169-0138.20.10.172.